

# The measurement of the dielectronic recombination in He-like Fe ions

H Watanabe<sup>1</sup>, F J Currell<sup>1,2</sup>, H Kuramoto<sup>1</sup>, Y M Li<sup>3</sup>, S Ohtani<sup>1,3</sup>,  
**B O'Rourke<sup>1,2</sup> and X M Tong<sup>1</sup>**

<sup>1</sup> Cold Trapped Ions Project, ICORP, Japan Science and Technology Corporation (JST), Tokyo 182-0024, Japan

<sup>2</sup> Queen's University, University Road, Belfast BT7 1NN, UK

<sup>3</sup> University of Electro-communications, Tokyo 182-8585, Japan

Received 24 July 2001, in final form 29 October 2001

Published 10 December 2001

Online at [stacks.iop.org/JPhysB/34/5095](http://stacks.iop.org/JPhysB/34/5095)

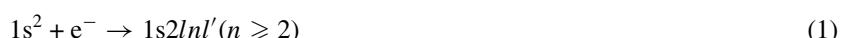
## Abstract

We have studied the dielectronic recombination process in He-like Fe ions and have obtained the resonant strengths of the  $KLn$  ( $3 \leq n \leq 5$ ) resonances. This measurement was performed with the use of an electron beam ion trap by measuring the x-ray energy emitted from highly charged ions simultaneously with the electron beam energy scanned during the measurement. The total resonant strengths obtained are  $5.0 \times 10^{-19}$ ,  $2.1 \times 10^{-19}$  and  $1.1 \times 10^{-19} \text{ cm}^2 \text{ eV}$ , for KLM, KLN and KLO, respectively.

## 1. Introduction

The dielectronic recombination (DR) process has been observed in high-temperature plasmas such as fusion plasmas and solar flares. Since this process is very fast in comparison with other processes occurring in plasmas and, thus, affects the charge balance in plasmas, this process has an importance for the study of astrophysics and plasma physics. In particular, iron (Fe) is an important element, since this is abundant in solar plasmas and exists in fusion plasmas as an impurity. Therefore the understanding of the DR process of Fe ions is important.

In the DR process a free electron is captured and a bound electron is simultaneously excited to form a doubly-excited state resonantly. Thereafter this state decays by photon emission. For example, in the case of He-like ions the doubly-excited state is produced as



which is the inverse of an Auger process. The produced state decays not by electron emission, but by photon emission through either of the two decay channels:



or



The DR process is specified by labels KLL, KLM and so on. For example, KLM means that a free electron is captured to the M shell (or L shell) and simultaneously the K electron is excited to the L shell (or M shell).

The studies of the DR process in He-like ions have been performed for several elements, because of their importance due to the closed-shell configuration. Ali *et al* [1, 2] reported the DR cross sections for He-like Ar ions by measuring the dependence of extracted ions on the electron beam energy with an electron beam ion source (EBIS). The measurements of the other elements such as Ar, Fe, Ni, Kr, Mo and Ba [3–7] were performed with the use of an electron beam ion trap (EBIT). In an EBIT the electron–ion interaction energy can be controlled arbitrarily by changing the acceleration voltage of the electron beam. Moreover, the energy width of the electron beam energy is narrow (about several tens of eV). The EBIT is a suitable device for studies concerned with the interaction between electrons and highly charged ions such as the DR process. In the measurements of Ar, Ni, Kr, Mo and Ba, DR resonances were observed by measuring x-ray spectra and the electron beam energy which was scanned during the measurements simultaneously [3, 4, 6, 7]. The satellite lines from the DR process in He-like Fe ions were measured by Beiersdorfer *et al* [5]. They measured x-rays using a crystal spectrometer, obtaining higher resolution than other studies. They resolved each resonant line in the KLL resonance and determined their resonant strengths. They also measured dielectronic satellite lines by the  $1s2lnl'(n \geq 3) \rightarrow 1s^2nl'$  transitions with a crystal spectrometer [8].

In this study we have measured the DR process in He-like Fe ions using a method in which both the x-ray energy and the electron beam energy were measured simultaneously during the scan of the electron beam energy. We obtained the total resonant strengths of  $KLn$  ( $3 \leq n \leq 5$ ). This result is compared with the results measured previously.

## 2. Experimental details

The measurement was performed with the Tokyo-EBIT [9, 10]. The electron beam emitted from an electron gun was accelerated with a potential difference between the trap region and the electron gun, during which the electron beam was compressed by a 4 T magnetic field produced with superconducting magnets. The trap region consists of three coaxial cylindrical electrodes called drift tubes, which are labelled DT1, DT2 and DT3 from the electron-gun side. In DT2 ions were trapped radially by the electrostatic potential produced by the electron beam and axially by the positive potential applied to both the DT1 and the DT3 with respect to DT2. Ions and atoms were electron impact ionized in a stepwise fashion by the electron beam until highly charged ions were produced. The light from ions was observed from an observation port through a  $2 \times 10$  mm slit in DT2.

The source Fe ions were introduced from a metal vapour vacuum arc (MEVVA) ion source placed at the top of the EBIT. The acceleration potential of the MEVVA was 4 kV and, thus, the DT2 potential was set to be 4 kV, during the ion injection, with respect to the earth potential. The potential of the electron gun was fixed at  $-4.5$  kV with respect to the earth. Therefore the electron beam energy was 8.5 keV. He-like Fe ions were cooked by keeping the beam energy at this value for 150 ms. The ionization energy of Li-like ions is 2.0 keV, while that of He-like ions is 8.8 keV. Thus He-like ions were by far the most dominant species trapped. From this cooking energy at 8.5 keV the electron beam energy was ramped linearly to 4.3 keV which was lower than the KLL resonant energy, and then returned to the cooking energy to produce He-like ions again. This sweep was fast enough (3 ms) to preserve the charge balance during the observation. A dump of trapped ions was performed every 3 s to avoid accumulation of unwanted ions, such as Ba ions, in the trap. The ion injection was also performed with this

period. Between the ion injections the cooking–observation cycle was performed 750 times. The electron beam current was 100 mA for all measurements.

During the scan of the electron beam energy, x-rays were measured with a Ge solid-state detector. The signal was taken into a computer by a multi-parameter data acquisition system [11], in which both the electron beam energy and the x-ray energy were recorded simultaneously in a list mode.

### 3. Theory

We have performed a theoretical calculation to obtain resonant energies and resonant strengths. In the calculation an isolated resonance approximation was used. Since the width of the resonances is narrow, the resonant strengths are commonly used instead of the cross sections. The resonant strengths are obtained by integrating the cross sections over the energy. If we designate the initial states as  $i$ , the intermediate doubly-excited states as  $d$  and the final states as  $f$ , the resonant strength is written in atomic units as

$$S_{idf} = \int_0^\infty \sigma_{idf}^{DR}(E) dE = \frac{\pi^2}{E_{di}} \frac{g_d}{2g_i} \frac{A_{di}^a A_{df}^r}{\sum A^a + \sum A^r} \quad (4)$$

where  $\sigma^{DR}(E)$  is the DR cross section,  $g_i$  and  $g_d$  are statistical weights of  $i$  and  $d$ , respectively,  $A_{df}^r$  is the rate of radiative transition from  $d$  to  $f$ ,  $A_{di}^a$  is the rate of autoionization from  $d$  to  $i$  and  $E_{di}$  is the resonant energy. The atomic structure parameters were calculated using the Hartree–Fock method with multiconfiguration relativistic corrections. The wavefunctions of continuum states were obtained with the distorted wave approximation method. To compare the theoretical result with the experimental one, the theoretical resonant strengths were convoluted with the energy profile of the electron beam which is approximated by normalized Gaussian functions:

$$\sigma_i^{DR}(E) = \sum_d \sum_f S_{idf} \frac{1}{\Delta \sqrt{\pi}} \exp \left[ -\frac{(E - E_{di})^2}{\Delta^2} \right] \quad (5)$$

where  $\Delta = w/(2\sqrt{\ln(2)})$ .  $w$  is the energy width of the electron beam.

The light observed may be polarized, since the excited states are produced with a directional electron beam. In our study the observations were performed at right angles with respect to the electron beam axis. Therefore, if the light is polarized, the observed intensity is not proportional to the total intensity emitted in all directions. This causes errors in the experimental resonant strengths. The polarization of emissions by DR was studied theoretically by Inal and Dubau [12]. For each resonance, the polarization degree can be calculated with equation (13) in their paper, when the energy levels of the intermediate doubly-excited states are isolated from each other. In our measurement the transition lines could not be resolved due to the width of the electron beam energy. The polarization degree was estimated with the use of the calculated polarization degrees together with the theoretical resonant strengths. The errors in the experimental resonant strengths originating from the neglect of the polarized line emissions are small (estimated to be less than 3.4%). This is because all lines are positively polarized by almost the same magnitude.

### 4. Results and discussion

A three-dimensional plot of the DR spectrum, obtained during a 75 min accumulation, is shown in figure 1. The background measured without the source ions injected has been subtracted in the preparation of this figure. The sharp peaks are the DR resonances. The feature due to

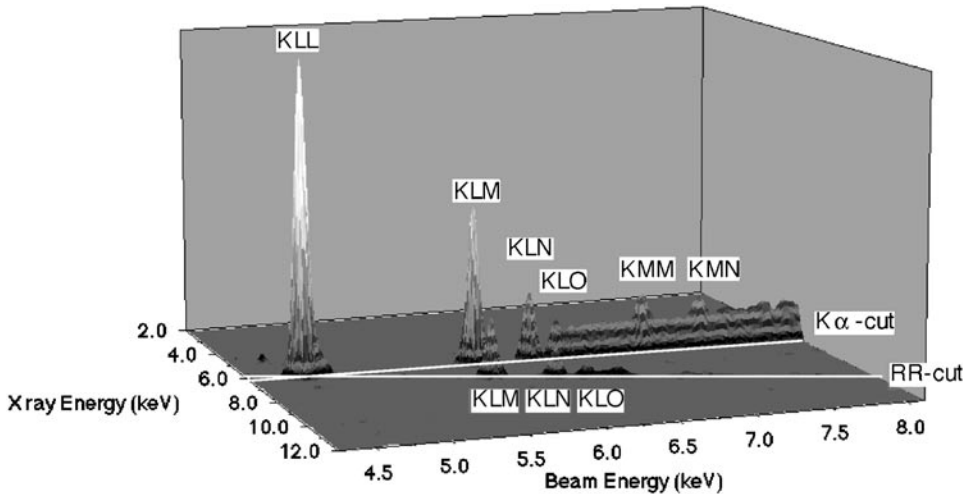
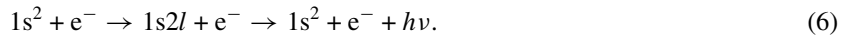


**Figure 1.** A surface plot of the spectrum obtained in the measurement. The x-rays indicated by ‘K $\alpha$ -cut’ are due to the  $n = 2 \rightarrow 1$  transition, while those indicated by ‘RR-cut’ correspond to the RR to  $n = 2$  in Li-like ions. The peaks in the figure are due to DR.

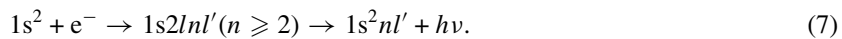
x-rays corresponding to the  $n = 2 \rightarrow 1$  transition energy is indicated as the ‘K $\alpha$ -cut’ (the process shown in figure 2(a)). This cut runs parallel with respect to the beam energy axis, since x-ray energy from a bound–bound transition is constant. The feature due to x-rays with the same energy as radiative recombination (RR) to  $n = 2$  to form Li-like ions is shown as the ‘RR-cut’ (the process shown in figure 2(b)). The x-ray energy due to RR changes linearly with the electron beam energy, since the x-ray energy is the sum of the beam energy and the ionization energy. As a result, the RR-cut forms a slanted line in this figure. As noted before, there are two decay channels after the production of doubly-excited states. If the inner electron decays to  $n = 1$  (i.e.  $n = 2 \rightarrow 1$ ), the resonance is observed on the K $\alpha$ -cut. The resonances observed on the RR-cut are due to the decay of the outer electron to  $n = 1$ . In this case, since both the initial and final states are the same as for nonresonant RR, the x-rays due to DR and RR are observed at the same position.

The x-ray energy axis was determined with x-ray lines from isotopes of Am and Co. The beam energy axis was determined from the x-ray axis with a RR line from the  $E_{\text{beam}} = E_{\text{x-ray}} - I_p$  relation, where  $E_{\text{beam}}$ ,  $E_{\text{x-ray}}$  and  $I_p$  are the electron beam energy, the x-ray energy and the ionization energy of Li-like Fe ions, respectively. The beam energy axis is displaced about 90 eV from theoretical values, perhaps due to an error originating from the weak intensity of the RR line. We shifted this axis to match theoretical values to compare the results.

Figures 3 and 4 are obtained by the projection of the K $\alpha$ -cut and the RR-cut onto the beam energy axis, respectively. The spectrum in figure 4 has been corrected for the energy dependence of the x-ray transmission of the Be window at the observation port. In figure 3 the x-ray above the electron impact excitation threshold arises from the direct electron impact excitation followed by a photon emission:



The peaks observed below the threshold are due to the DR process corresponding to



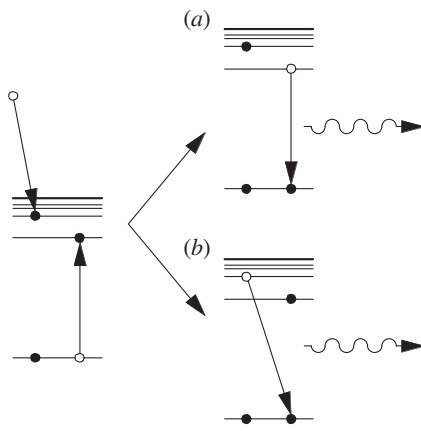


**Figure 2.** (a) The DR process observed on the  $K\alpha$ -cut. The x-rays from DR observed on this cut originate from the  $n = 2 \rightarrow 1$  transition by the inner electron. (b) The DR process observed on the RR-cut. The x-rays from DR on this cut arise from the transition by the outer electron. The x-ray energy by this process is the same as that from RR, since both the initial and final states are the same.

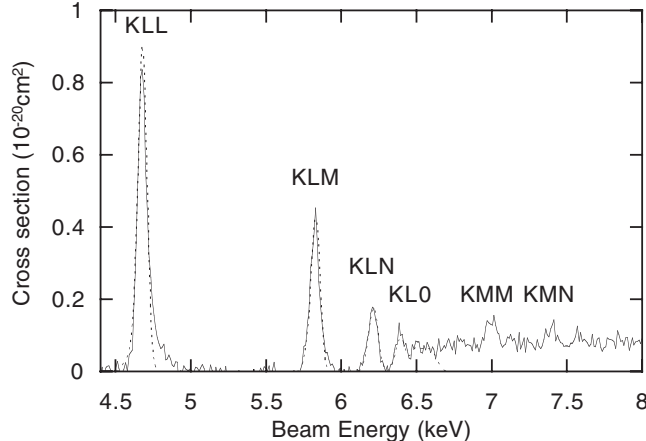
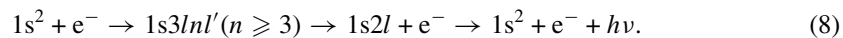
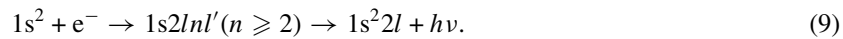


**Figure 3.** The spectrum obtained by the projection of the  $K\alpha$ -cut onto the beam energy axis. The solid curve indicates the experimental result, while the dotted curve indicates the spectrum synthesized from the theoretical result. In the theoretical result the doubly-excited configurations up to  $n = 10$  are considered.

The peaks indicated by KMM and KMN on the background due to x-rays produced after the direct excitation are due to resonant excitation, where an electron is captured to form a doubly-excited state followed by the autoionization producing a singly-excited state. These states decay by photon emission. This process is shown as



In figure 4 the DR resonances appear along the RR-cut, corresponding to



The ordinate in figures 3 and 4 is the cross section ( $10^{-20} \text{ cm}^2$ ). Since the RR process is the inverse of photoionization, the RR cross section can be calculated precisely.

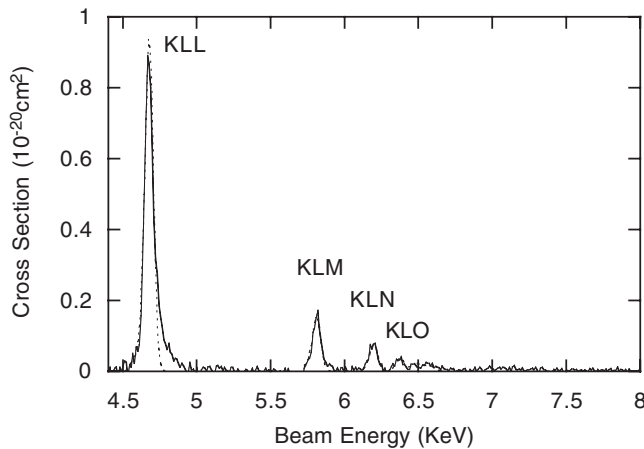


**Figure 4.** The spectrum obtained by the projection of the RR-cut onto the beam energy axis. The solid curve indicates the experimental result, while the dotted curve indicates the theoretical one. In the theoretical result the doubly-excited configurations up to  $n = 10$  are considered.

Moreover RR is observed simultaneously with DR in the spectrum measured by this type of experiment. Normalization to the RR intensity is sometimes performed to determine the absolute value of the ordinate [4, 6, 7]. However, because of the weak intensity of RR this procedure could not be used in this study. Therefore instead of RR, we used the KLL resonant strength measured by Beiersdorfer *et al* [5] for the normalization. Since they measured the resonant strengths of each resonant line, we summed over their results to obtain the resonant strength of the KLL resonance. The result was  $7.4 \times 10^{-19} \text{ cm}^2 \text{ eV}$ . It was noted that the absolute uncertainty in the value for each resonant line was 20%. By summing over these uncertainties in quadrature the uncertainty of 9.3% was obtained. We determined the ordinate such that the area enclosed by the KLL resonance is the same as the value shown above. The cross sections of KLL are slightly different in figures 3 and 4. This is due to the fitting errors occurring in determination of the area corresponding to the KLL resonance.

Since the energy width of DR is narrow, it can be considered that the width of resonances originates from that of the electron beam energy. The width of the electron beam energy is determined by fitting Gaussian functions to the KLL resonance. The obtained result is about 60 eV FWHM, so we consider this value as the width of the electron beam energy. With this value, the calculated resonant strengths and energies, and equation (5), the theoretical spectra are calculated. In figures 3 and 4 the theoretical cross sections are shown at the same time. The agreement between theory and experiment is quite good. The small difference in the high-energy tail of the KLL resonance may originate from lower-charge-state ions such as Li-like and Be-like ions. Neglecting their contribution causes an error of 4.2% in the experimental resonant strengths.

We obtain the resonant strengths of  $KLn$  resonance by integrating the areas enclosed by the peaks. These results are listed in table 1. The errors shown in the table are estimated from those in the results of Beiersdorfer *et al* [5], the errors originating from polarization and the statistical error in our result. The errors due to the contamination of lower-charge-state ions are also included in the errors.

The resonant strengths of  $KLn$  resonances in He-like ions have been measured for several elements. The result of the present study is compared with those which have been reported previously. The results are shown in figure 5. The data on the KLL resonance of Fe in the

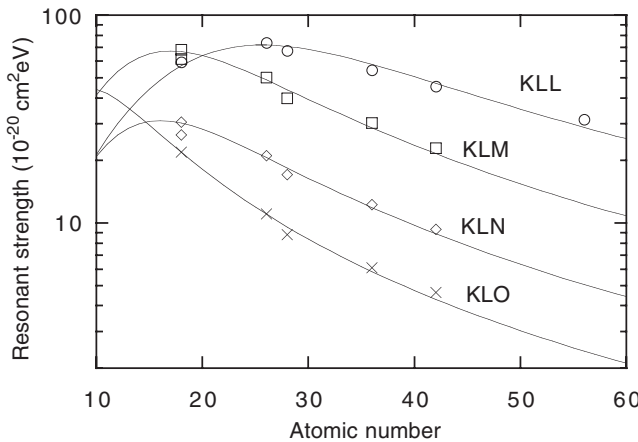


**Figure 5.** The comparison of the total DR resonant strengths of He-like ions. The data for  $\text{Ni}^{26+}$ ,  $\text{Mo}^{40+}$  and  $\text{Ba}^{54+}$  were obtained by Knapp *et al* [6], those for  $\text{Kr}^{34+}$  by Fuchs *et al* [7] and those for  $\text{Ar}^{16+}$  by Ali *et al* [2] and by Smith *et al* [4]. The data for  $\text{Fe}^{24+}$  are our results, though the value of the KLL resonance is from Beiersdorfer *et al* [5].

**Table 1.** The resonant strengths of DR of He-like Fe ions measured in this study. The values in the parentheses are experimental uncertainties. The branching ratios are also shown.

Resonance	$1s2lnl' \rightarrow 1s^2nl'$ ( $10^{-20} \text{ cm}^2 \text{ eV}$ )	$1s2lnl' \rightarrow 1s^22l'$ ( $10^{-20} \text{ cm}^2 \text{ eV}$ )	Total ( $10^{-20} \text{ cm}^2 \text{ eV}$ )
KLM	37.7(4.0) 75%	12.5(1.4) 25%	50.2(4.2)
KLN	15.7(1.8) 74%	5.4(0.8) 26%	21.1(2.0)
KLO	9.0(1.3) 82%	2.0(0.4) 18%	11.0(1.4)

figure are from Beiersdorfer *et al* [5]. Their result was obtained using a crystal spectrometer and measuring spectra at fixed electron beam energies. In their measurement each resonant line in the KLL resonance was resolved and their resonant strengths were obtained. The result of Ali *et al* [2] was obtained by measuring the charge balance in the EBIS with extracted ions. The absolute values were obtained by considering the equilibrium of a rate equation in conjunction with the theoretical electron impact ionization cross section of Li-like ions. The other measurements used a method almost the same as ours [4, 6, 7]. In these measurements, however, absolute values of spectra were obtained by normalization using the RR line intensities and the theoretical RR cross sections. The results of Knapp *et al* [6] and Fuchs *et al* [7] are theoretical values which were verified by their own experiments. As seen in the figure, our result is consistent with those expected from the previous results.

The radiative transition rate  $A^r(Z)$ , the autoionization rate  $A^a(Z)$  and the energy  $E(Z)$  scale as  $A^r(Z) = Z^4 A^r(H)$ ,  $A^a(Z) = A^a(H)$  and  $E(Z) = Z^2 E(H)$ , respectively [13], where  $H$  means the nonrelativistic hydrogenic value. With equation (4), the resonant strengths may be scaled as

$$S = \frac{1}{m_1 Z^2 + m_2 Z^{-2}} \quad (10)$$

where  $m_1$  and  $m_2$  can be calculated from nonrelativistic hydrogenic wavefunctions. The curves in figure 5 show a trend of measured resonant strengths with the atomic number, with the use

**Table 2.** The parameters  $m_1$  and  $m_2$  in equation (10). The values in the parentheses are a measure of the error in the parameters.

Resonance	$m_1$ ( $10^{15}$ cm $^{-2}$ eV $^{-1}$ )	$m_2$ ( $10^{20}$ cm $^{-2}$ eV $^{-2}$ )
KLL	1.06(6)	4.55(47)
KLM	2.56(15)	2.15(24)
KLN	6.25(36)	4.12(46)
KLO	13.2(7)	0.95(90)

of equation (10). The values of  $m_1$  and  $m_2$  are listed in table 2. The uncertainties quoted in the table are derived from the fitting procedure based on experimental uncertainties to give a rough guide to the errors associated with the parameters  $m_1$  and  $m_2$ . For the results of Knapp *et al* [6] and Fuchs *et al* [7], experimental uncertainties are also used as the measure of the errors in their results. Further benchmarked measurements are needed over a wide range of atomic numbers to improve the uncertainties in the parameters  $m_1$  and  $m_2$ .

The ratios of the  $1s2lnl' \rightarrow 1s^2nl' + h\nu$  channel with respect to all the decay channels of the doubly-excited states produced in the DR process are estimated from the experimental result. These ratios are 75% for KLM, 74% for KLN and 82% for KLO. 70–85% of all the doubly-excited states decay by the  $1s2lnl' \rightarrow 1s^2nl' + h\nu$  channel.

## 5. Conclusions

We measured x-ray emission due to the DR process in He-like Fe ions with the Tokyo-EBIT and determined the resonant strengths. From our result the resonant strengths are  $5.0 \times 10^{-19}$ ,  $2.1 \times 10^{-19}$  and  $1.1 \times 10^{-19}$  cm $^2$  eV, for KLM, KLN and KLO respectively. The ratios for the decay of the  $1s2lnl' \rightarrow 1s^2nl' + h\nu$  channel with respect to all the decay channels of the doubly-excited states are 75, 74 and 82% for KLM, KLN and LNO, respectively. We performed theoretical calculations and compared them with our experimental results. The agreement is good. Moreover the present result is consistent with that expected from the results measured previously.

## Acknowledgments

This work was performed under the auspices of the International Cooperative Research Project (ICORP) of the Japan Science and Technology Corporation. We are grateful to the Royal Society and the Great Britain Sasakawa Foundation for additional funding which made the travel associated with this collaboration possible.

## References

- [1] Ali R, Bhalla C P, Cocke C L and Stockli M 1990 *Phys. Rev. Lett.* **64** 633
- [2] Ali R, Bhalla C P, Cocke C L, Schulz M and Stockli M 1991 *Phys. Rev. A* **44** 223
- [3] Smith A J, Beiersdorfer P, Decaux V, Widmann K, Reed K J and Chen M H 1996 *Phys. Rev. A* **54** 462
- [4] Smith A J, Beiersdorfer P, Widmann K, Chen M H and Scofield J H 2000 *Phys. Rev. A* **62** 052717
- [5] Beiersdorfer P, Phillips T W, Wong K L, Marrs R E and Vogel D A 1992 *Phys. Rev. A* **46** 3812
- [6] Knapp D A, Marrs R E, Schneider M B, Chen M H, Levine M A and Lee P 1993 *Phys. Rev. A* **47** 2039
- [7] Fuchs T, Biedermann C, Radtke R, Behar E and Doron R 1998 *Phys. Rev. A* **58** 4518
- [8] Beiersdorfer P, Schneider M B, Bitter M and von Goeler S 1992 *Rev. Sci. Instrum.* **63** 5029
- [9] Currell F J *et al* 1996 *J. Phys. Soc. Japan* **65** 3186
- [10] Watanabe H *et al* 1997 *J. Phys. Soc. Japan* **66** 3795
- [11] Currell F J *et al* 1997 *Phys. Scr. T* **73** 371
- [12] Inal M K and Dubau J 1989 *J. Phys. B: At. Mol. Opt. Phys.* **22** 3329
- [13] Cowan R D 1981 *The Theory of Atomic Structure and Spectra* (Berkeley, CA: University of California Press)